Journal of the Korean Crystal Growth and Crystal Technology
Vol. 15, No. 2 (2005) 51-56

Synthesis of orthorhombic $LiMnO_2$ and its electrochemical properties

Jung-Min Kim and Hoon-Taek Chung†

Department of Ceramic Engineering, Faculty of Engineering, Dongshin University, Chonnam 520-714, Korea

(Received February 17, 2005)
(Accepted March 2, 2005)

Abstract We prepared orthorhombic $LiMnO_2$ by emulsion drying method. The thermo-gravimetric measurement and X-ray diffraction studies indicated that the orthorhombic $LiMnO_2$ phase was formed above 800°C by oxygen evaporation process from $LiMn_2O_4$ and Li_2MnO_3. In this process, we could control the ordering of $LiMnO_2$ with heating rate. It was observed that electrochemical properties depended on the ordering of this material; the ordered one exhibited good capacity retention, whereas the disordered one suffered capacity fading upon cycling, especially in the 3 V region. Transmission electron microscopic (TEM) study showed that this difference is related with difference in the stress relieving effects in the samples.

Key words $LiMnO_2$, Orthorhombic, Cathode, Li-ion Battery, Emulsion

1. Introduction

The layered intercalation compounds such as $LiCoO_2$ [1], $LiNiO_2$ [2] and $LiMnO_2$ [3] have been intensively investigated as cathode materials for lithium-ion secondary battery. Among them, the $LiMnO_2$ system has several advantages over $LiCoO_2$ and $LiNiO_2$ such as low cost, less toxic and abundance of Mn source.

Orthorhombic $LiMnO_2$ (space group of Pmnm, hereafter referred to o-$LiMnO_2$), which has a zigzag layered β-$NaMnO_2$ structure, is expected to be a promising cathode material for Li-ion secondary battery due to its high theoretical capacity, 285 mAh/g. However, o-$LiMnO_2$ transforms irreversibly from orthorhombic phase to spinel-like one during several initial cycles, and then it subsequently transforms again from cubic structure to tetragonal structure upon cycling, which is consistent with appearance of two plateaus at around 4 and 3 V vs. Li [4-9]. As a result, o-$LiMnO_2$ shows much better cycling performances than spinel $LiMn_2O_4$ at room and elevated temperatures, even after it converts to spinel-like phase.

Previous research group proposed that low-temperature solution technique seems to be necessary to obtain high capacity [10]. It was also proposed that the electrochemical behavior of o-$LiMnO_2$ is improved by stacking faults (structural disorder) and small crystalline size [11, 12]. Recently, Jang *et al.* [13, 14] reported that a well-ordered o-$LiMnO_2$ synthesized by freeze-drying method at 950°C shows high-capacity retention upon cycling. By means of TEM observation, they suggested that the reason of capacity retention upon cycling is that the anti-phase domains in spinel-like structure generated from o-$LiMnO_2$ by cycling are able to accommodate the Jahn-Teller induced strain which is one of the reasons of capacity fading. As described above, we could expect that the structural disorder would be one of the factors effecting on electrochemical properties of o-$LiMnO_2$.

In our previous reports, we could prepare fine particle size of cathode materials such as $LiMn_2O_4$ [15] and $LiCoO_2$ [16]. Therefore, we adopted emulsion drying method to synthesize o-$LiMnO_2$ with small particle. In this study, we investigated the powder electrochemical properties of o-$LiMnO_2$ prepared by emulsion drying method.

2. Experimental

The $LiMnO_2$ precursor was prepared by emulsion drying method using a mixture of aqueous solution of $LiNO_3$ (Kanto, 99 %) and $Mn(NO_3)_2{\cdot}6H_2O$ (Kanto, 98 %) (1 : 1 mol ratio). The detailed powder preparation route well described in previous report [15]. The obtained emulsion-dried gel-like precipitates was burned about 300°C, and then burned-out powder was heated again at 400°C for 1 h in air (hereafter the heated powders referred as to precursor). The precursor was calcined at various temperatures for 12 h in Ar atmosphere.

In order to investigate the thermal behavior of the precursor, thermo-gravimetric measurement was performed at the rate of 10°C min^{-1} in the temperature range from room temperature to 950°C under Ar flowing. The pre-

†Corresponding author
Tel: +82-61-330-3183
Fax: +82-61-330-3173
E-mail: htchung0710@hanmail.net

pared powders were characterized by X-ray diffractometer. The FWHMs (full width at half maximum) of several peaks for each powder were measured from the XRD patterns. Transmission electron microscopy (TEM) observations were carried out by using as-synthesized o-$LiMnO_2$ and electrochemically cycled powders. The powders were ultrasonically de-agglomerated and dispersed on Cu grid for TEM observation.

For electrochemical testing, cathode slurry was fabricated by mixing the prepared o-$LiMnO_2$ powder, acetylene black and polyvinylidene fluoride in a weight ratio of 75 : 15 : 10 in N-methly-2-pyrolidinone. The slurry was pasted on nickel ex-met (1 cm^2) and dried at 120°C for 2 days in a vacuum, and then the cell was assembled in an argon-filled glove box. This cell consisted of the cathode as the working electrode, lithium ribbon of 0.35 mm thickness as the counter electrode, and 1 M $LiClO_4$ in a propylene carbonate as an electrolyte. Electrochemical tests performed on the cell using WBCS3000 (XENO, Korea) between 2.0 and 4.3 $V_{Li/Li+}$ at a constant current density of 20 mA/g at 30°C.

3. Results and Discussion

3.1. Powder preparation

A stoichiometric mixture of emulsion-dried gel-like precipitates was burned at 300°C, resulting to powder. And, the burned-out powder was heated again at 400°C for 1 h in air to remove the residual oil components such as Kerosene and Tween 85. Figure 1 shows TGA result of the precursor under Ar flowing to 950°C. The observed weight loss of the precursor mainly consists of three

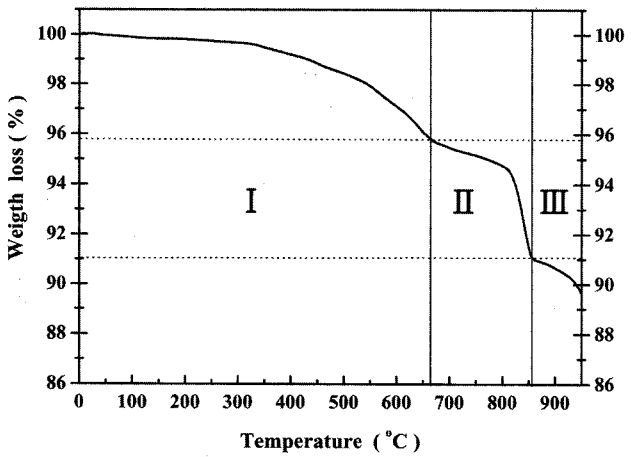

Fig. 1. Thermo-gravimetric measurement of precursor under Ar flow to 950°C.

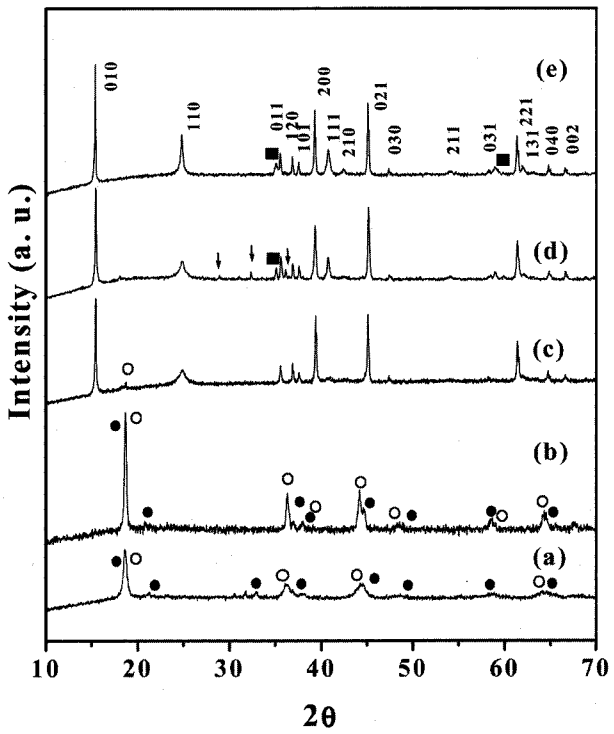

Fig. 2. X-ray diffraction patterns of (a) precursor, (b) calcined at 650°C, (c) sample A, (d) sample B and (e) sample C. Hollow circle, solid circle, the arrow and solid square represent spinel $LiMn_2O_4$, Li_2MNO_3, Mn_3O_4 and MnO, respectively.

stages. In region I, there is a gradual weight loss to 650°C. It is well known that the heat-treatment of Li-Mn-O compound at 400°C in air results in oxygen rich spinel phase which is observed in Fig. 2a. Firing at 650°C for 12 h in Ar atmosphere brought about clear two mixtures, $LiMn_2O_4$ and Li_2MnO_3, which means that the temperature below 650°C is not enough to form o-$LiMnO_2$. In region II, two kinds of weight losses are observed. The first progressive weight loss is also considered as oxygen evaporation, leading to $LiMn_2O_{4-\delta}$ and $Li_2MnO_{3-\delta}$. Then, a drastic oxygen loss (ca. 3.8 wt%) from the both compounds would give rise to o-$LiMnO_2$ at temperature around 825~850°C. As can be seen in Fig. 2c, calcination of the precursor at 825°C brought about a well-defined crystallization of o-$LiMnO_2$, which coincides well with the TGA result. The possible reaction routes are represented as follow;

Region I) $LiMnO_{2+\delta} \rightarrow LiMn_2O_4 + Li_2MnO_3 + xO_2$ (650°C)

Region II) $LiMn_2O_4 + Li_2MnO_3 \rightarrow LiMn_2O_{4-\delta} + Li_2MnO_{3-\delta} + xO_2$ (650~800°C)

$LiMn_2O_{4-\delta} + Li_2MnO_{3-\delta} \rightarrow 3LiMnO_2 + xO_2$ (800~850°C)

Further weight loss in Region III is due mainly to the evaporation of lithium ingredient and reduction of manganese oxides. As confirmed by XRD patterns in Figs. 2d and e, calcination at 850°C gave secondary phases such as Mn_3O_4 and MnO owing to the evaporation of lithium and reduction of manganese oxides. From TGA and XRD studies, it would be thought that the o-$LiMnO_2$ phase was formed by oxygen evaporation process from $LiMn_2O_4$ and Li_2MnO_3.

The pristine powders were observed by TEM and illustrated in Fig. 3. All samples showed a typical rect-

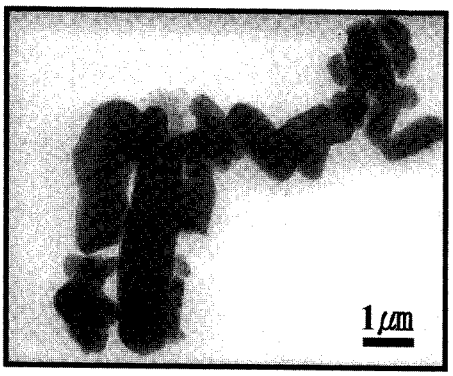

(a)

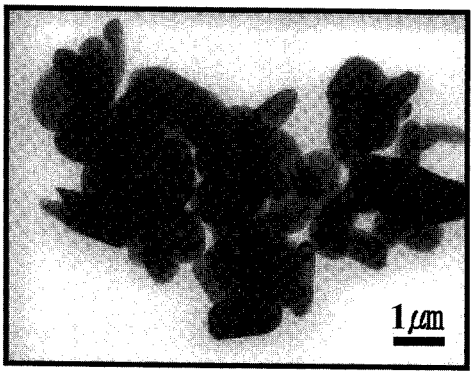

(b)

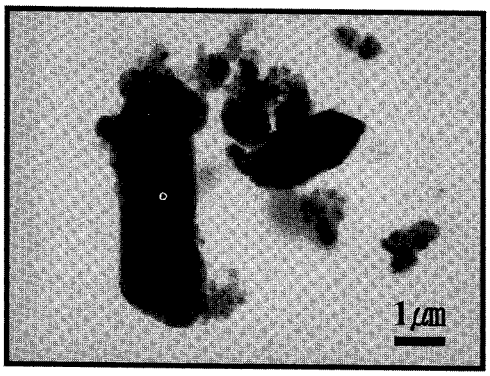

(c)

Fig. 3. TEM images of pristine particles for (a) sample A, (b) sample B and (c) sample C.

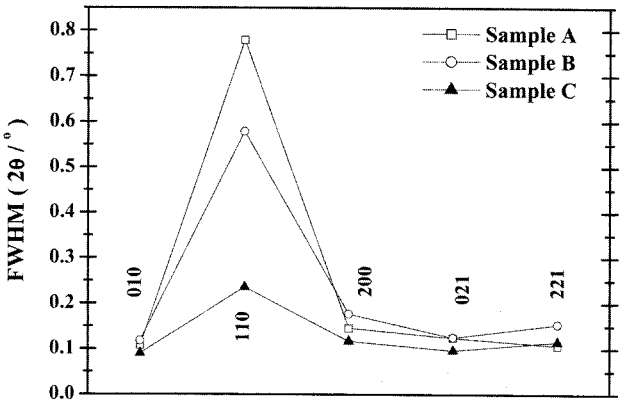

Fig. 4. Full width at half maximum of several peaks for each samples measured from XRD patterns.

angular type of particle shape, which is usually observed in o-$LiMnO_2$ system. The measured average particle size is 1~2 μm in all samples.

From XRD patterns of Fig. 2, FWHMs were measured by collecting several peaks. There is a remarkable variation in the FWHMs of the (110) Bragg peak. The measured value decreased with increasing calcination temperature as well as reducing heating and cooling rates. The others of FWHMs of diffraction peaks remain nearly constant irrespective of calcination conditions. The observed changes in the FWHM means a degree of disorder that is directed toward monoclinic structure as reported by Croguennec *et al.* [17]. And, they suggested that this disorder of o-$LiMnO_2$ gives different electrochemical properties [11]. From this result, it is expected that sample C may show good electrochemical properties.

3.2. Electrochemistry

Electrochemical properties of the prepared powders were examined on the range from 2.0 to 4.3 V vs. Li applying current density of 20 mA/g at 30°C. Figure 5 shows the initial charge and several discharge curves of samples as a function of specific capacity vs. voltage. Sample A shows the highest charge capacity of about 172 mAh/g due probably to its spinel impurities as observed by XRD in Fig. 2c. Sample B and C show somewhat lower initial capacity than that of sample A. Regardless of the divergence in their the first charge, discharge capacity of all samples drastically falls on the first charge due to the phase transformation from the orthorhombic to spinel-like structure, and the obtained capacity gradually increases by further cycling. As shown in Fig. 5, both 4 and 3 V plateaus increase in all samples correlated with lithium insertion in tetrahedral

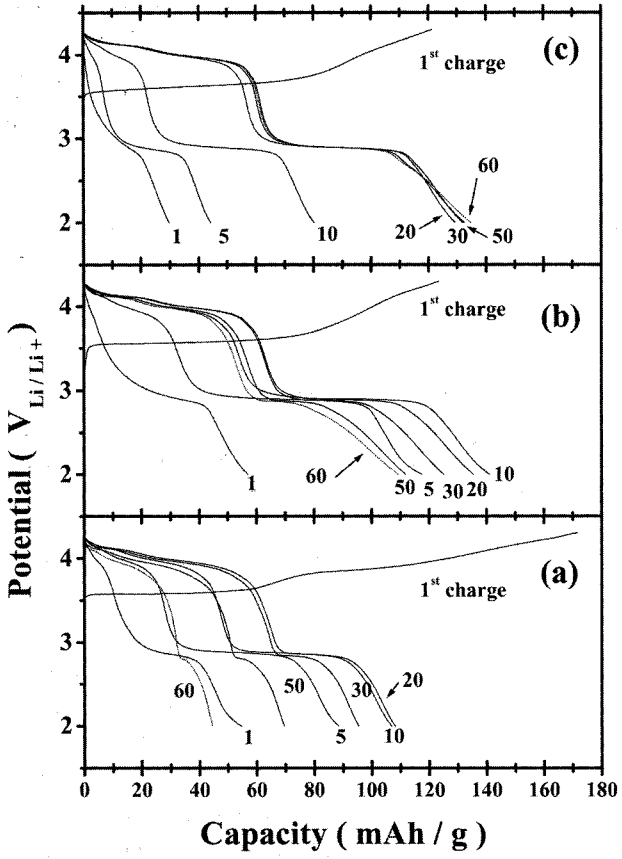

Fig. 5. The first charge and several discharge curves of (a) sample A, (b) sample B and (c) sample C as a function of specific capacity vs. potential.

8a and octahedral 16c sites in spinel-like structure, respectively. These mean that the phase transformation occurs in all samples upon cycling [13]. Figure 5 also shows the different trends of cycling behavior for each sample during cycling. It is likely that an ordered orthorhombic $LiMnO_2$ (sample C) needs more cycle to show the highest capacity upon cycling [5].

Figure 6 shows capacities of the samples during 80 cycles. After the first charge, it is observed that the capacities of all samples fall abruptly and then gradually increase to form spinel-like structure [13]. Although highly disordered sample A delivered a high initial charge capacity, the capacity fading occurs at early cycle, and it do not recover its initial charge capacity. Sample B exceeds its initial capacity but it also shows capacity fading by further electrochemical cycling. Whereas ordered sample C delivers highest capacity and good capacity retention among samples. From these results, we can safely conclude that the ordered o-$LiMnO_2$ shows good capacity retention than the disordered phase one as we expected in Fig. 4.

We divided the obtained discharge capacity down into 4 and 3 V regions up to 60 cycles as shown in Figs. 7a and b, respectively. The disordered phases show capacity fading on both 4 and 3 V regions and the capacity fading of 3 V region is severe than that of 4 V region. However, the ordered phase (sample C) shows no capacity fading on both 3 and 4 V regions. In case of spinel

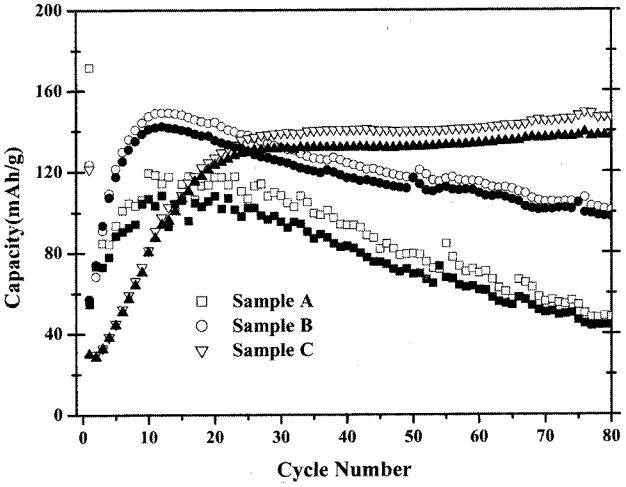

Fig. 6. Charge and discharge capacities of each sample up to 80 cycles. White and black represent charge and discharge capacity, respectively.

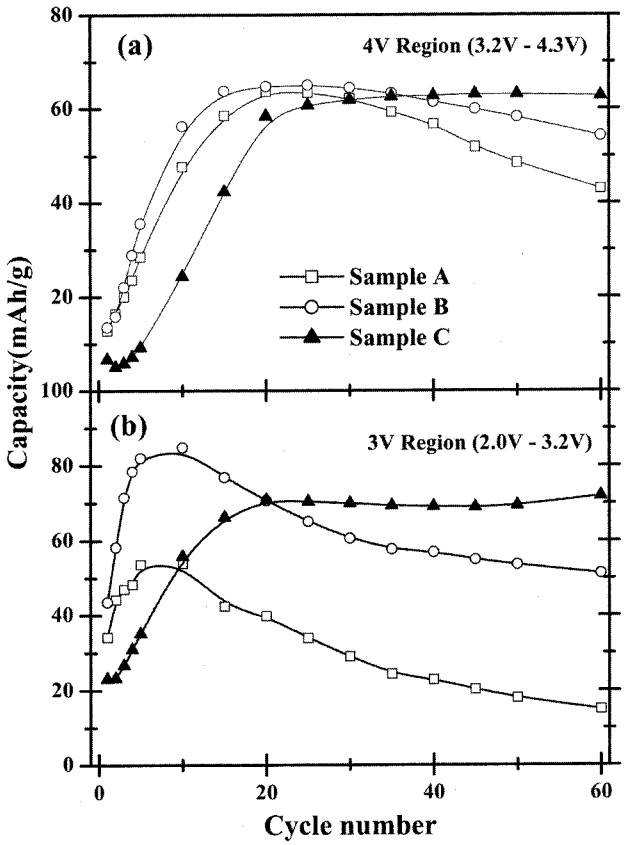

Fig. 7. Discharge capacities of (a) 4 V and (b) 3 V region for each sample up to 60 cycles.

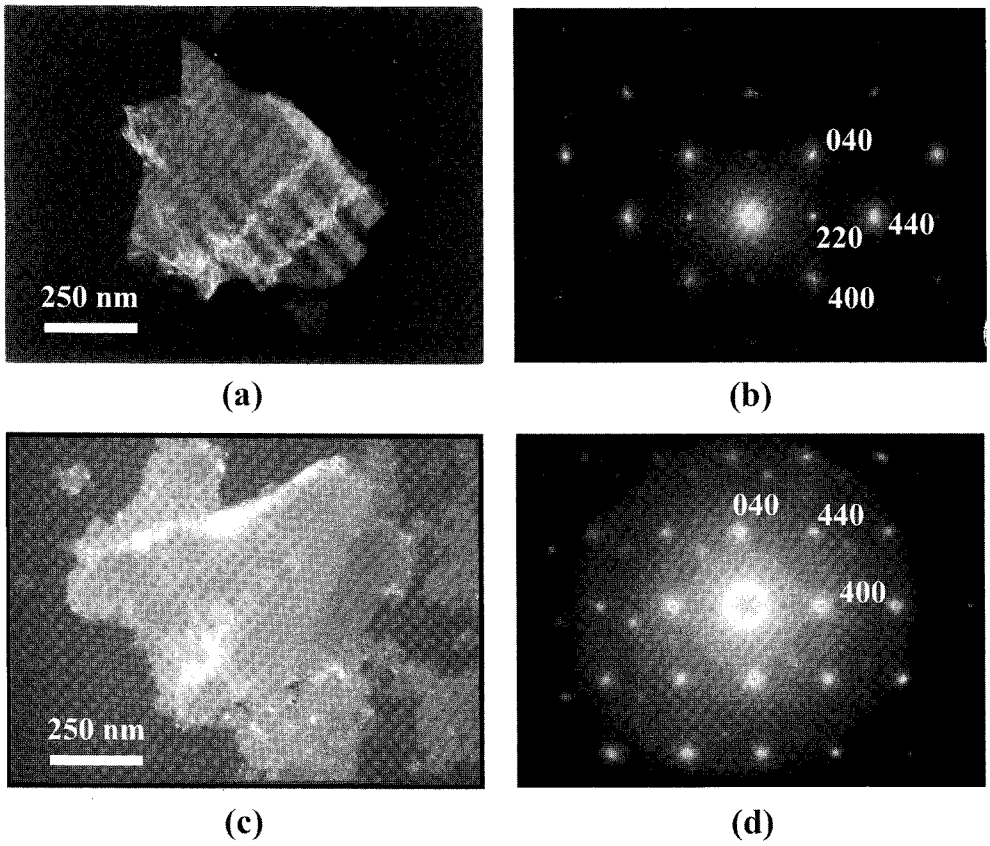

Fig. 8. TEM images of extensively cycled particle for samples B (a) dark field and (b) SAD pattern ([001] zone axis) and for sample C (c) dark field and (d) SAD pattern ([001] zone axis).

$LiMn_2O_4$, it is well known that Li^+ ions are inserted into 16c octahedral sites of the spinel structure at 3 V region, which is accompanied by a huge structural volume change about 16 % caused by a Jahn-Teller distortion. On contrast, electrochemically formed spinel-like structure generally shows better capacity retention than spinel $LiMn_2O_4$. Wang *et al.* [14] suggested that the anti-phase domains in spinel-like structure generated from $LiMnO_2$ by electrochemical cycling are able to accommodate the Jahn-Teller strain. In our electrochemical experimental results, the disordered phases show severe capacity fading at 3 V region like the spinel $LiMn_2O_4$, but the ordered phase shows no capacity fading.

TEM observations were carried out for the sample B and C after 80 cycles. Figure 8 shows dark field images of samples and their selected area diffraction (SAD) patterns. Although the cubic and tetragonal structures have nearly the same SAD pattern, the cubic structure can be easily recognized by detecting the (220) reflection in the [001] zone axis [19]. Figure 8b, the SAD pattern of sample B shows that it seems has only a cubic structure after cycling. However, the SAD pattern of sample C shows that it has both tetragonal and distorted spinel structure in the particle. Electrochemical experiments and TEM observations indicate that sample C (ordered $LiMnO_2$) could tolerate more the strain in the particle than sample B (disordered $LiMnO_2$). Therefore, it is likely that the ordered phase accommodates its the strain caused by huge volume changing during cycling in its structure due probably to the existence of anti-phase domains in spinel-like structure as can be seen Fig. 8c. However, it seems from the TEM image in Fig. 8a that the anti-phase domains might be not exist in the sample B after extensive cycling because the particle was severely damaged and fractured by electrochemical cycling. We previously reported that particle disruption could be one of the reasons of capacity fading of spinel $LiMn_2O_4$ upon cycling [18]. Therefore, it is thought that particle disruption derived from disordered $LiMnO_2$ would be one of the reasons of capacity fading for electrochemically formed spinle-like structure from o-$LiMnO_2$.

4. Conclusion

We successfully synthesized o-$LiMnO_2$ powders cal-

cined in Ar atmosphere from the emulsion-dried precursor. TGA and XRD studies revealed that o-$LiMnO_2$ was formed by oxygen loss from rock salt type of Li_2MnO_3 and spinel type of $LiMn_2O_4$ between 650°C and 850°C. From electrochemical results, it was found that the capacity fading mainly occurred at 3 V region on disordered phase and the ordered phase shows better capacity retention both 3 and 4 V regions after transformation to spinel-like structure. It is expected that the ordered o-$LiMnO_2$ phase may show good electrochemical properties. It seems from the TEM observations that the ordered phase accommodates its the strain caused by huge volume changing during cycling in its structure due probably to the existence of anti-phase domains in the electrochemically formed spinel-like structure. Whereas the particle of disordered phase was severely damaged and fractured by electrochemical cycling. Therefore, it is concluded that structural disorder is one of the factors of effecting on electrochemical properties of o-$LiMnO_2$.

Acknowledgements

This work was supported by Dongshin University. Authors are grateful for this supporting.

References

[1] K. Mizushima, P.C. Jones, P.J. Wiseman and J.B. Goodenough, "Li_xCoO_2 ($0<x<-1$): A new cathode material for batteries of high energy density", Mater. Res. Bull. 15 (1980) 783.

[2] C. Delmas and I. Saadoune, "Electrochemical and physical properties of the $Li_xNi_{1-y}Co_yO_2$ phases", Solid State Ionics 53 (1992) 370.

[3] A.R. Armstrong and P.G. Bruce, "Synthesis of $LiMnO_2$ as an electrode for rechargeable lithium batteries", Nature 381 (1996).

[4] I.J. Davidson, R.S. McMillan, J. J. Murray and J.E. Greedan, "Lithium-ion cell based on orthorhombic $LiMnO_2$", J. Power Sources 54 (1995) 232.

[5] L. Groguennec, P. Deniard and R. Brec, "Electrochemical cyclability of orthorhombic $LiMnO_2$. Characterization of cycled materials", J. Electrochem. Soc. 144 (1997) 3323.

[6] M.M. Thackeray, "Structural considerations of layered and spinel lithiated oxides for lithium ion batteries", J. Electrochem. Soc. 142 (1995) 2558.

[7] W. Tang, H. Kanoh and K. Ooi, "Lithium ion extraction from orthorhombic $LiMnO_2$ in ammonium peroxodisulfate solutions", J. Solid State Chem. 142 (1999) 19.

[8] R.J. Gummow, D.C. Liles and M.M. Thackeray, "Lithium extraction from orthorhombic lithium manganese oxide and the phase transformation to spinel", Mater. Res. Bull. 28 (1993) 1249.

[9] I.M. Kotschau and J.R. Dahn, "*In situ* X-ray study of $LiMnO_2$", J. Electrochem. Soc. 145 (1998) 2672.

[10] J.N. Reimers, E.W. Fuller, E. Rossen and J.R. Dahn, "Synthesis and electrochemical studies of $LiMnO_2$ prepared at low temperatures", J. Electrochem. Soc. 140 (1993) 3396.

[11] L. Groguennec, P. Deniard, R. Brec and A. Lecerf, "Preparation, physical and structural characterization of $LiMnO_2$ samples with variable cationic disorder", J. Mater. Chem. 5 (1995) 1919.

[12] L. Groguennec, P. Deniard, R. Brec, P. Biensan and M. Broussely, "Electrochemical behavior of orthorhombic $LiMnO_2$: influence of the grain size and cationic disorder", Solid State Ionics 89 (1996) 127.

[13] Y.I. Jang, B. Huang, H. Wang, D.R. Sadoway and Y.M. Chiang, "Electrochemical cycling-induced spinel formation in high-charge-capacity orthorhombic $LiMnO_2$", J. Electrochem. Soc. 146 (1999) 3217.

[14] H. Wang, Y.I. Jang and Y.M. Chiang, "Origin of cycling stability in monoclinic- and orthorhombic-phase lithium manganese oxide cathodes", Electrochem. and Solid-State Lett. 2 (1999) 490.

[15] S.T. Myung and H.T. Chung, "Preparation and characterization of $LiMn_2O_4$ powders by the emulsion drying method", J. Power Sources 84 (1999) 32.

[16] S.T. Myung, N. Kumagai, S. Komaba and H.-T. Chung, "Preparation and electrochemical characterization of $LiCoO_2$ by the emulsion drying method", J. Appl. Electrochem. 30 (2000) 1081.

[17] L. Groguennec, P. Deniard, R. Brec and A. Lecerf, "Nature of the stacking faults in orthorhombic $LiMnO_2$", J. Mater. Chem. 7 (1997) 511.

[18] S.T. Myung, H.T. Chung, S.H. Komaba, N. Kumagai and H.B. Gu, "Capacity fading of $LiMn_2O_4$ electrode synthesized by the emulsion drying method", J. Power Sources 90 (2000) 103.

[19] M.M. Thackeray, Y. Shao-Horn, A.J. Kahaian, K.D. Kepler, E. Skinner, J.T. Vaughey and S.A. Hackney, "Structural fatigue in spinel electrodes in high voltage (4 V) $Li/Li_xMn_2O_4$ cells", Electrochem. and Solid-State Lett. 1 (1998) 7.